HHS Public Access

Author manuscript

IEEE Trans Neural Syst Rehabil Eng. Author manuscript; available in PMC 2018 May 01.

Published in final edited form as:

IEEE Trans Neural Syst Rehabil Eng. 2017 May ; 25(5): 447–458. doi:10.1109/TNSRE.2016.2577882.

Anatomical Directional Dissimilarities in Tri-axial Swallowing Accelerometry Signals

Faezeh Movahedi,
Department of Electrical and Computer Engineering, Swanson School of Enginering, University of Pittsburgh, Pittsburgh, PA, USA

Atsuko Kurosu,
Department of Communication Science and Disorders, School of Health and Rehabilitation Sciences, University of Pittsburgh, Pittsburgh, PA, USA

James L. Coyle,
Department of Communication Science and Disorders, School of Health and Rehabilitation Sciences, University of Pittsburgh, Pittsburgh, PA, USA

Subashan Perera, and
Department of Medicine, Division of Geriatric Medicine, University of Pittsburgh, Pittsburgh, PA, USA

Ervin Sejdić
Department of Electrical and Computer Engineering, Swanson School of Enginering, University of Pittsburgh, Pittsburgh, PA, USA

Abstract

Swallowing accelerometry is a non-invasive approach currently under consideration as an instrumental screening test for swallowing difficulties, with most current studies focusing on the swallowing vibrations in the anterior-posterior (A-P) and superior-interior (S-I) directions. However, the displacement of the hyolaryngeal structure during the act of swallowing in patients with dysphagia involves declination of the medial-lateral (M-L), which suggests that the swallowing vibrations in the M-L direction have the ability to reveal additional details about the swallowing function. With this motivation, we performed a broad comparison of the swallowing vibrations in all three anatomical directions. Tri-axial swallowing accelerometry signals were concurrently collected from 72 dysphagic patients undergoing videofluoroscopic evaluation of swallowing (mean age: 63.94 ± 12.58 years period). Participants swallowed one or more thickened liquids with different consistencies including thin-thick liquids, nectar-thick liquids, and pudding-thick liquids with either a comfortable self-selected volume from a cup or a controlled volume by the examiner from a 5ml spoon. Swallows were grouped based on the viscosity of swallows and the participant's stroke history. Then, a comprehensive set of features was extracted in multiple signal domains from 881 swallows. The results highlighted inter-axis dissimilarities among tri-axial swallowing vibrations including the extent of variability in the amplitude of signals, the

Correspondence to: Ervin Sejdić.

degree of predictability of signals, and the extent of disordered behavior of signals in time-frequency domain. First, the upward movement of the hyolaryngeal structure, representing the S-I signals, were actually more variable in amplitude and showed less predictable behavior than the sideways and forward movements, representing the A-P and M-L signals, during swallowing. Second, the S-I signals, which represent the upward movement of the hyolaryngeal structure, behaved more disordered in the time-frequency domain than the sideways movement, M-L signals, in all groups of study except for the pudding swallows in the stroke group. Third, considering the viscosity and the participant's pathology, thin liquid swallows in the non-stroke group presented the most directional differences among all groups of study. In summary, despite some directional dissimilarities, M-L axis accelerometry characteristics are similar to those of the two other axes. This indicates that M-L axis characteristics, which cannot be observed in videofluoroscopic images, can be adequately derived from the A-P and S-I axes.

Index Terms

Tri-axial swallowing accelerometry; cervical auscultation; dysphagia; signal processing

I. INTRODUCTION

SWALLOWING is a complex neuromuscular process requiring a series of biomechanical events, which result in the safe passage of liquids and solids from mouth to the stomach without entering the airway [1], [2]. Due to the complexity of the swallowing process, many health complications, such as radiation therapy for head/neck cancers, and neurological disorders, like strokes, can affect the swallowing function. Dysphagia, swallowing disorders, can affect any of the four stages of swallowing. Serious and potentially fatal health consequences associated with dysphagia negatively impact the health, safety, and quality of life of patients [3], [4]. Aspiration, dehydration, and malnourishment are probable complications of dysphagia [5]–[8]. Approximately 1 in 25 adults in the United States will have a swallowing problem annually [9]. Moreover, studies have shown that dysphagia is prevalent among the elderly population due to age-related effects on swallowing physiology in addition to age-related diseases [3], [4], [7], [10]–[12].

There are two primary imaging instrumental examinations used for diagnosis and management of dysphagia: videofluoroscopic swallow studies (VFSS) and fiberoptic endoscopic swallowing tests (FEES) [13]–[16]. VFSS, which has been considered the gold standard of dysphagia testing for over 30 years [13], [14], consists of radiographic imaging of the structure and the biomechanical functions of the upper aerodigestive tract during the ingestion of different consistencies of barium coated materials, and how the swallowed material (bolus) flows through the oral and pharyngeal cavities [14], [17]. However, VFSS is not always available or feasible, and asymptomatic patients are routinely not referred for a VFSS because they do not display overt signs of dangerous or disordered swallowing function. VFSS also requires an examiner with specialized clinical expertise and the use of a radiology suite, which may be unavailable in some areas. [13], [18]. Early identification of dysphagia through screening tests has received much attention in the past 10 years. These efforts have attempted to accomplish two goals. First, the screening is designed to

preemptively identify dysphagia before patients with impaired protection of the airway are put in harm's way and are allowed to orally ingest food and liquids. Second, the screening identifies the patients in need of gold-standard imaging testing with VFSS or FEES and identifies those who do not need the expensive testing. When the screening tests are used precisely according to protocol, they possess reasonable sensitivity for identifying dysphagia or its absence in symptomatic patients. However, since they rely on human observation of the overt signs of dysphagia (coughing or choking while eating or drinking), they completely fail to identify patients without overt signs of dysphagia who are at risk for dysphagia. Moreover, adherence to the published screening protocols has not been universally good due to clinical expediency. Therefore, there has been a growing interest in complementary dysphagia screening methods that provide high accuracy, are non-invasive and easy to administer by minimally trained individuals, and consume few resources in healthcare institutions.

Many studies have recently considered the use of swallowing accelerometry for dysphagia screening. Swallowing accelerometry is based on the measurement of vibrations recorded in the upper aerodigestive tract structure during the act of swallowing [19]–[22]. Numerous investigations have been performed in attempt to find the physiological sources of swallowing vibrations. Some of the studies have considered the displacement of the hyoid bone and larynx as a physiological source of swallow signals [17], [19]. The displacement of hyoid bone is an essential component of the swallowing function that contributes to the protection of the airway during the swallow, as well as, the traction forces necessary to distend the upper esophageal sphincter and allow the flow of swallowed material into the digestive portion of the mechanism [1], [19], [23]–[25].

The final goal of the swallowing accelerometry method is to classify healthy swallows and unhealthy swallows based on swallowing vibrations recorded by accelerometers. To reach this goal, at the first step, we should be able to characterize swallowing vibrations by extracting various features that provide us crucial information about swallowing. Some studies investigated simple features from swallowing signals in time-domain such as onset of swallows, duration of swallows, timing of the different physiological stages of the swallow, and the magnitude of signals [19], [26]–[30]. On the other hand, some studies have extracted advanced features in time, frequency, and time-frequency domains from swallow vibrations [26], [31]–[34]. The results from past studies have shown the validity of the swallowing accelerometry method's use of one or two directions of anterior-posterior (A-P) and superior-inferior (S-I), representing the forward and upward movements of hyolaryngeal structures during swallowing, in swallow classification and capturing swallowing difficulties [22], [26], [31], [32], [35], [36]. While the focus of most studies was on the assessing performance of different classification methods based on computed features, few studies have directly compared extracted features in two directions of A-P and S-I to find out about the dissimilarities between the swallowing vibrations in different anatomical directions [22], [36]–[38]. The results have showed that both of the A-P and S-I axes contain different temporal and spectral information about swallowing. Their findings indicated that the employment of two axes of the dual-accelerometer in swallowing accelerometry analysis would be beneficial as each axis provides unique information about swallowing. However, it should be mentioned that the focus of previous researches were on healthy subjects [22],

[36]–[38], rather than unhealthy subjects who suffering from dysphagia, even though the ultimate goal of swallowing accelerometry is to catch any swallowing difficulties in patients who have or are at the risk of dysphagia. No study has comprehensively compared features of swallowing signals in the A-P and S-I directions under various conditions such as swallowing different volumes and viscosities in subjects who suffer from swallowing difficulties. It should be also mentioned that the selection of features in previous studies were subjective, as there is no clear answer to which features probably characterize the two directions of swallow vibrations. In addition, previous studies utilized different procedural methods, which limits the ability to compare their results. Therefore, there is still a need of further investigation about swallowing vibrations in both the A-P and S-I axes to have a better understanding of swallowing in different anatomical directions. While most attention to swallowing-related movements of hyolaryngeal structures has been to their S-I and A-P directions, both of which are clearly observed with VFSS, little to no attention has been directed to medial-lateral (M-L) movements. It is plausible that hyolaryngeal movement in the M-L plane occurs due to the origins and the insertions of paired muscles responsible for displacing the hyolaryngeal complex and the selective, asymmetrical weakening of these muscles in disease states such as certain types of stroke, cranial nerve injury, maxillofacial trauma, head and neck resections, and others [39], [40]. Therefore, due to the interesting observations that arose when a second axis of recording was added to single-axis accelerometry, the addition of the final, third axis (M-L) may provide intriguing information about the relationship of swallowing accelerometry signals to actual biomechanical swallowing activity, particularly in patients with diseases affecting symmetry of hyolaryngeal muscle contractions.

While most attention to swallowing-related movements of hyolaryngeal structures has been to their S-I and A-P directions, both of which are clearly observed with VFSS, little to no attention has been directed to medial-lateral (M-L) movements. It is plausible that hyolaryngeal movement in the M-L plane occurs due to the origins and the insertions of paired muscles responsible for displacing the hyolaryngeal complex and the selective, asymmetrical weakening of these muscles in disease states such as certain types of stroke, cranial nerve injury, maxillofacial trauma, head and neck resections, and others. Therefore, due to the interesting observations that arose when a second axis of recording was added to single-axis accelerometry, the addition of the final, third axis (M-L) may provide intriguing information about the relationship of swallowing accelerometry signals to actual biomechanical swallowing activity, particularly in patients with diseases affecting the symmetry of hyolaryngeal muscle contractions.

The purpose of this study is to comprehensively compare of tri-axial swallowing accelerometry signals in both stroke and non-stroke subjects while examining various viscosities amongst the three anatomical directions. The main question in this study is to examine whether accelerometry signals derived from different anatomical planes provide discriminate information about swallowing function. To answer this question, nine features in time, information-theoretic, frequency, and time-frequency domains have been extracted from tri-axial swallowing accelerometry signals from dysphagic patients. The outcome of this study provides insights into how using tri-axial accelerometers can be helpful to identify swallowing difficulties. In addition, the possible effect of age and gender on the differences

between the values of the extracted features in the three directions has been investigated in this study.

II. METHODOLOGY

A. Data Acquisition

72 patients (mean age 63.94 ± 12.58 years, 42 male, 30 female), who underwent videofluoroscopic examinations at the Presbyterian University Hospital of the University of Pittsburgh Medical Center (Pittsburgh, Pennsylvania), participated in this study. There were 20 patients who had a previous history of stroke as the reason behind their swallowing difficulties (a neuromuscular issue), while the other 52 patients had other various reasons such as radiation therapy for head/neck cancer or other anatomical issues. All participants signed informed consent and the data collection protocol was approved by the University of Pittsburgh Institutional Research Board. As a part of their examinations, the participants swallowed one or more thickened liquids with different consistencies including thin-thick liquid (Varibar Thin Liquid with < 5 cPs viscosity), nectar-thick liquid (Varibar Nectar with ≈300 cPs viscosity), and pudding-thick liquid (Varibar Pudding with ≈5000 cPs viscosity). The viscosity of boluses changed for each patient based on the speech pathologists' decision considering different factors, such as patients' condition at the time of examinations, patients' history including stroke history, diet, and any specific health considerations. Participants performed the swallows in a neutral head position and, in some cases, in a head-flexion ("chin-tuck") position, which has been used in dysphagia patients to prevent aspiration during swallowing [41]. Swallows with swallow maneuvers, such as the supraglottic swallow, Mendelsohn maneuver, and effortful swallow, were eliminated from the study. In this study, each swallow was rated on an accepted 8-point ordinal clinical Penetration-Aspiration (PA) scale to determine the severity of swallowing difficulty in patients, and we included swallows within all range of severity ($1 < PAscore < 8$). Since the purpose of this study was to determine whether tri-axial accelerometry provided additional information that characterizes swallow physiology compared to dual-axis accelerometry, there was no specific limitation regarding the severity of dysphagia because the event of interest was the physiology of the swallow event.

881 swallows were recorded with a tri-axial accelerometry (ADXL 327, Analog Devices, Norwood, Massachusetts) with a sensitivity of 420mV/g, resolution of 250 $\mu g/\sqrt{Hz} rms$, and an acceleration measurement of a minimum full-scale range of ±2g. Previous studies have shown that the optimal cervical placement for digital detectors to record the swallowing sounds and vibrations is on the midline of the cricoid cartilage [21], [34], [42]. The sensor was taped to the participants' anterior neck at the level of the cricoid cartilage, such that the sensitive axes of the accelerometer were aligned to the anatomical anterior-posterior (A-P), superior-inferior (S-I), and medial-lateral (M-L) axes, as shown in Fig. 1. Signals from the A-P, S-I, and M-I axes were bandpass filtered from 0.1 to 3000 Hz and amplified (model P55, Grass Technologies, Warwick, Rhode Island) prior to storage on a research computer. The voltage signals for each axis of the accelerometer were fed into a National Instruments 6210 DAQ and recorded at 20 kHz by the LabView program Signal Express (National Instruments, Austin, Texas). Concurrent with the accelerometer recordings, the

biomechanical activity and the bolus flow in the upper aerodigestive tract were captured by the x-ray machine (Ultimax system, Toshiba, Tustin, CA) at 30 pulses per second, and videofluoroscopic images were captured at 60 frames per second by a video card (AccuStream Express HD, Foresight Imaging, Chelmsford, MA) and recorded to a hard drive with the same Labview program.

B. Data Preprocessing

The time-marked vibration signals were collected with the tri-axial accelerometer in the S-I, A-P, and M-I directions. The time-linked onsets and offsets of each swallow were obtained via frame-by-frame temporal analysis videofluoroscopic images by a trained experience speech-language pathologist whose inter- and intra-rater reliability in the judgment of these parameters was established a priori. The onset of the swallow segments was defined as the time at which the leading edge of the presented bolus intersected with the shadow cast on the x-ray image by the posterior border of the ramus of the mandible. The offset was the time that the hyoid bone completed motion associated with swallowing-related pharyngeal activity and returned to its resting position. After segmentation of the swallow signals, they were grouped based on the two factors including the viscosity of the liquids participants were swallowing and whether the participants had a stroke history, since dysphagia following a stroke and the effects of viscosity on the swallowing signals have been well-documented [18], [29], [43]–[46]. Then, each swallow was pre-processed as follows. As the first step, the mechanical and electrical thermal noise created by the accelerometer was attenuated from the signal by applying axial-specific finite impulse response (FIR) filters [37]. We first fitted an auto-regressive (AR) model to the output of the accelerometer without any input and then use the coefficients of the AR model to generate the FIR filter. In the next step, the low frequency components associated with head movement were attenuated from the signals using a least-squares spline approximation algorithm [47], [48]. We fitted a low-frequency (< 2 Hz) trend to the time-domain signal and then subtracted that low-frequency trend from the time-domain recording. In the last step, to reduce the impact of both white and colored noise on a given signal, the filtered signals were denoised via a ten-level discrete wavelet transform using the Meyer wavelet with soft thresholding. The level of decomposition was determined by minimizing noise in the signal while retaining the interesting detail of the signals [49]. Figure 2 illustrates the swallowing signals before and after applying signal processing techniques.

C. Feature Extraction

To capture key statistical differences between swallowing vibration in the A-P, S-I, and M-L axes, several features in multiple domains were extracted from each of the axes of each swallow signal. In this study, 9 features in time, information-theoretic, frequency, and time-frequency domains were evaluated. Further, the practicality of these features had already been demonstrated in previous swallowing signal studies [22], [31], [32], [37], [50]. The computational details for each of these features are described in the following subsections.

1. *Time Domain Features:* To find out whether the physics of signal behavior differs between the different anatomical axes of accelerometer, a number of time

domain features are computed for the swallowing vibrations. Considering a signal $X = \{x_1, x_2, \ldots x_n\}$, the following features are extracted:

- The unbiased estimation of the standard deviation can be obtained as

$$\sigma_X = \sqrt{\frac{1}{n-1}\sum_{i=1}^{n}(x_i - \mu_X)^2} \quad (1)$$

  where μ_X denotes the mean of the signal. The standard deviation reflects how the signal fluctuates around the mean value. Here the important parameter is the ac signal power represented by the deviation from the mean. The bigger the standard deviation, the wider the distribution of data points.

- Skewness quantifies how symmetrical the amplitude distribution is. This feature can be computed as follows:

$$\xi_X = \frac{\frac{1}{n}\sum_{i=1}^{n}(x_i - \mu_X)^3}{\{\frac{1}{n}\sum_{i=1}^{n}(x_i - \mu_X)^2\}^{\frac{3}{2}}} \quad (2)$$

  A symmetrical distribution has a skewness of zero. Whereas an asymmetrical distribution with a long tail to either the right or left has a positive or negative skew, respectively.

- Kurtosis is a measure of whether the amplitude distribution is peaked or flat relative to a normal distribution. A high kurtosis value tends to have a distribution with a sharp, narrow peak, declines rather rapidly, and has heavy tails, while a low kurtosis value signifies a distribution with a flattened peak and has thin tails [51]. This feature is computed as:

$$\gamma_X = \frac{\frac{1}{n}\sum_{i=1}^{n}(x_i - \mu_X)^4}{\{\frac{1}{n}\sum_{i=1}^{n}(x_i - \mu_X)^2\}^{2}} \quad (3)$$

2. *Information-Theoretic Features:* The information-theoretic features are popular metrics for characterizing biological signals. The different genres of information-theoretic features are summarized below.

   - The Lempel-Ziv complexity (LZC) is a practical tool to evaluate the randomness of finite sequences, well-suited for physiologic signals [52], [53]. To calculate the LZC, a signal has to be first transformed into

a symbolic sequence, since LZC measures complexity through an estimated number of distinct patterns obtained by parsing a symbolic sequence [53]. Quantization is a typical method used to convert biomedical signals into a binary sequence. The signal is converted to 100 symbols by comparing it to 99 thresholds. After the quantized signal is obtained, it can be decomposed into the k blocks. Then, the LZC calculated as:

$$LZC=\frac{K\log_{100}n}{n} \quad (4)$$

The logarithm of n, signal length, to the base 100 is used in the above formula as the signal is quantized into 100 symbols.

- The entropy rate is useful to compare the degree of regularity of the signal distribution [46], [54], [55] between the S-I, A-P, and M-L axes. Zero and one values of entropy rate indicate a periodic repetition of the same pattern and aperiodic dynamics, respectively. First, to normalize values of X, μ_X is subtracted from X and divided by σ_X. Then, it is quantized into 10 equally spaced levels. In the next step, sequences of consecutive points in quantized signal $\hat{X}$ of length H, $10 \leq H \leq 30$, are coded as a series of integers, $\Upsilon_H = \{u_1, u_2, \ldots u_{n-H+1}\}$, by means of the following formula:

$$u_i=10^{H-1}\hat{x}_i+H-1+10^{H-2}\hat{x}_i +H-2+\ldots+10^0\hat{x}_i \quad (5)$$

Now the normalized entropy rate is computed as

$$\tilde{\Delta}(H)=\frac{\Delta(H)+\Delta(H-1)+\Delta(1)perc(H)}{\Delta(1)} \quad (6)$$

where *perc(H)* is the percent of unique occurrence of coded integers in the sequence of H and $\Delta_{(H)}$ is the calculated Shannon entropy of the sequence which is obtained as follows:

$$\Delta_{(H)}=\sum_{q=0}^{10^H-1} P\Upsilon_H(q)\ln P\Upsilon_H(q) \quad (7)$$

Finally, entropy rate is presented as ρ, an index of regularity

$$\rho=1-min(\tilde{\Delta}(H)) \quad (8)$$

3. *Frequency Domain Features:* Three features in frequency domain were considered in this study mentioned below. First, the fast Fourier transform of the signal was computed to measure the frequency domain features.

   - Peak frequency is simply the frequency corresponding to maximum power and is computed as follows:

$$f_p = \arg_{f\in[0,f_{max}]} max|F_X(f)|^2 \quad (9)$$

     where $f_{max} = 100Hz$.

   - The spectral centroid was evaluated as:

$$\hat{f} = \frac{\int_0^{f_{max}} f|F_X(f)|^2 df}{\int_0^{f_{max}} |F_X(f)|^2 df} \quad (10)$$

   - The bandwidth of the signal is defined as follows:

$$BW = \sqrt{= \frac{\int_0^{f_{max}} (f-\hat{f})^2 |F_X(f)|^2 df}{\int_0^{f_{max}} |F_X(f)|^2 df}} \quad (11)$$

4. *Time-Frequency Domain Features:* Time-frequency features provide simultaneous descriptions of the signal in the time and frequency domains. Recently, the wavelet transform has been considered as a powerful technique for time-scale analysis of a signal and has shown potential in biomedical signal processing [56]–[60]. It provides varying time-frequency resolution. Applying wavelet transform would have advantages since swallows produce non-stationary signals.

   - The concept of entropy was used in the current study to compare the disorderly behavior in swallowing signals in all three axes of the accelerometer: S-I, A-P, and M-L. The wavelet entropy was defined based on the wavelet transform. To perform a wavelet transform, a 10-level Meyer wavelet decomposition is applied to a swallow signal to compute the energy contained in different time-frequency bands. Considering d_k as a vector containing wavelet approximation coefficients at *kth* level of decomposition, the energy at the *kth* level is defined as

$$E_{d_k} = \|d_k\|^2 \quad (12)$$

where ‖•‖ means the Euclidean norm. In the next step, the relative wavelet energy equal to energy at a given decomposition level to the total energy of the signal was computed as

$$\Phi_{d_k} = \frac{E_{d_k}}{E_{a_{10}} + \sum_{k=1}^{10} E_{d_k}} \times 100\% \quad (13)$$

Φ_{d_k} gives valuable information regarding the energy distribution of the signal at different frequency bands. Finally, the wave entropy rate is computed as:

$$\Theta_X = -\Theta_{a_{10}} \log_2 \Theta_{a_{10}} - \sum_{k=1}^{10} \Theta_{d_k} \log_2 \Theta_{d_k} \quad (14)$$

The high/low value of Θ_X specifies disorder/order behavior of a signal.

Table 1 contains the summary of all features and their definitions.

D. Statistical Analysis

To account for multiple trials involving the same participants, linear mixed models with random effects were employed as an analytic strategy in this study. First, the anatomical direction differences were computed between three axes for all extracted features in each of the trials. Then, an intercept-only model was fitted to assess the statistical significance of each of the said differences in the presence of multiple trials per participant. Secondly, in order to identify the correlates of extracted features, another series of linear mixed models with each of the extracted features and their between anatomical differences (if applicable) as the dependent variable were fitted; each of the individual potential correlates age, gender, and participants' stroke history and them collectively as fixed effect(s) of interest; and a participant random effect. The statistical significance of the parameters of the fixed effects solution with interpretation analogous to regression coefficients were used as evidence of significant association. Due to the large number of extracted features examined and the opportunity for inflated type I error due to multiplicity, the false discovery rate (FDR) methodology was used to make multiplicity corrections to the p-values in all analyses. SAS version 9.3 (SAS Institute, Inc., Cary, North Carolina) was used for all statistical analyses in this study. The benchmark for statistical significance was established at $p < 0.05$.

III. Results

The accelerometer data were presented in this study for 72 participants including 881 swallows. A total number of 162 comparisons were made between the directional couples of (A-P & S-I), (M-L & S-I), and (A-P & M-L) for all extracted features. Here, we summarize statistically significant results.

A. Demographical Analysis

Before discussing the results of features computed in this study, it should be pointed out that statistical analysis shows no significant effects of age, gender, and participants' stroke history on directional comparisons of the computed features from tri-accelerometry swallowing signals.

B. Time Domain Analysis

Table 2 displays the results of time domain features calculated in this study for each of the A-P, S-I, and M-L axes, grouped by viscosity and by participants' stroke history. Firstly, it should be mentioned that the standard deviation (σ) showed directional dissimilarity in all groups of the study ($p < 0.02$). As we can see in Table 2, the S-I axes demonstrated the highest σ compared to the A-P and M-L in all groups of study.

In addition, considering the asymmetry of swallowing signals, ξ_s, the A-P amplitude distributions in non-stroke participants were mostly positively skewed; whereas the S-I amplitude distributions had a tendency to be strongly negatively skewed in both the thin ($p < 0.05$) and pudding ($p < 0.05$) groups. Furthermore, even though the signals in both the A-P and S-I axes in the non-stroke pudding group showed high kurtosis, the S-I signals were more meaningfully leptokurtic ($p = 0.03$), which resulted in a higher peak than the A-P signals. Other groups showed no statistical differences between the directions in swallow signals.

C. Information-Theoretic Analysis

The summary of information-theoretic features is presented in Table 3. The results for entropy rate ρ indicate the statistical differences between the anatomical axes in two cases. First, the entropy rate differed among all three directions of thin swallows in the non-stroke group ($p < 0.005$). In particular, the M-L axis for the thin non-stroke group had a greater entropy rate than the A-P ($p < 0.01$) and S-I ($p < 0.01$) signals. Secondly, the A-P entropy for nectar swallows in the non-stroke group was higher than the M-L entropy (p=0.0413).

Considering the evaluation of randomness in swallow signals, the statistical analysis for LZC presented the most directional differences among the extracted information-theoretic features in this study. As demonstrated in Table 3, the S-I signals exhibited larger LZC than M-L signals in all groups of study ($p < 0.005$), except within the thin stroke group and the nectar the non-stroke group. In addition, the LZC for the S-I signals was higher than for A-P signals in thin and nectar swallows in the stroke group and pudding swallows in the non-stroke group ($p < 0.01$).

D. Frequency Domain Analysis

Table 4 represents the summary of frequency features considered in the current study. The results for most of the groups showed no significant directional differences for peak frequencies (f) as well as centroid frequencies ($\hat{f}$), except for the following cases. First, considering pudding swallows in the stroke group, the A-P signals had significantly smaller peak frequencies than the S-I signals ($p < 0.01$) and greater peak frequencies than the M-L signals ($p < 0.05$). Moreover, the S-I signals had lower centroid frequencies than the A-P

signals for non-stroke pudding swallows ($p < 0.02$) and the M-L signals for stroke thin swallows ($p < 0.02$).

Additionally, the bandwidth of the A-P signals was considerably lower than for the M-L axis in the non-stroke group for thin and nectar swallows ($p < 0.03$), and for the thin viscosity in the stroke group ($p < 0.05$).

E. Time-Frequency Domain Analysis

In the time-frequency domain, the wavelet entropy rate (Θ_X) results for the three anatomical directions in stroke and non-stroke groups are represented in Table 5. The S-I signals had greater Θ_X than M-L signals for all cases ($p < 0.01$), except for pudding swallows in the stroke group.

F. Summary of All Findings

A total number of 198 comparisons were performed between the features calculated for the A-P, S-I, and M-L directions of swallowing signals and then grouped by the viscosity and participants stroke history. Among 198 directional comparison cases, only 47 cases showed directional differences, which is ≈ 24% of total number of comparisons. As we can see in Figure 4, the greatest percentage of directional dissimilarity was allocated to the standard deviation (37.5%), LCZ (16.67%) and wavelet entropy rate (14.59%).

Table 6 summarizes all of our findings. Each circle specifies the existing differences between the values of the computed features for the two directions. The rows and column that are highlighted in the orange and green colors indicate the features and the viscosity group, respectively, that presented the largest number of directional dissimilarities. First, we consider the features that give us the largest numbers of directional difference among the various groups of study. Results obtained for the standard deviation (SD), Lempel-Ziv complexity (LZC), and wavelet entropy rate features showed 18, 8, and 7 directional dissimilarities cases, respectively, representing ≈ 69% of the total dissimilarities. 36%, 34% and 30% of the directional differences were found in comparisons between S-I & A-P, S-I & M-L, and M-L & A-P, respectively. Generally, the S-I signals demonstrated higher values in SD, LZC, and wavelet entropy when comparing with M-L and A-P signals. Secondly, while considering the viscosity and the participants' stroke history, all groups of study showed the minimum 6 directional dissimilarities in measured features. Thin swallows in the non-stroke group demonstrated the most directional dissimilarities among all of the groups of study, as highlighted in light green in Table 6.

IV. Discussion

The present study provides a quantitative characterization of the three anatomical directions of swallowing signals recorded by a tri-axial accelerometer during videofluoroscopy in patients with swallowing difficulties. This is the first study to consider the M-L axis in swallowing signals recorded during simultaneous videofluoroscopic imaging. Multiple features in the time, information-theoretic, frequency, and time-frequency domains were extracted from the swallowing signals for each of the A-P, S-I, and M-L directions.

The efficiency of swallowing process is reduced with aging [61], [62], which that may be reflected in swallowing vibrations recorded by an accelerometer [38], [63]. However, in this study, age did not effect our results of directional variation, as it was neutralized by the relatively small age range of the study participants (72 participants with mean age of 63.94). In addition, we did not observe sex-related effects on our results. Although few studies have shown small sex-related differences in swallowing [38], [63] due to differences in the anatomy of the neck and throat between males and females [61], [62], [64], the absence of sex dependency in our study might be a result of applying different methodologies, and most importantly recruiting only unhealthy subjects suffering from swallowing difficulties that could like dissemble the effects of otherwise important features, i.e. biological sex.

Time-domain analysis showed that all swallow signals in three directions demonstrated a low standard deviation, low positive or negative skewness, and high kurtosis values indicating dense symmetrical distribution of swallow signals with amplitude values decreasing rapidly above and below the mean. The S-I signals had higher standard deviation values than the A-P and M-L signals, which indicates that the upward movement of the hyolaryngeal structure was actually more variable in amplitude than sideways and forward movements during swallowing. In addition, the A-P signals of pudding swallows in the non-stroke group showed higher values in skewness and kurtosis than the S-I signals. This suggests that the intensity of the forces in the forward direction was smaller for longer periods of time during swallows and had a peaked distribution when compared to vertically directed forces.

Based on the results of the information-theoretic features, the swallowing signals in the three directions demonstrated predictable and regular behavior, which is representative of the presence of periodic non-random patterns in swallowing signals, in all the groups of the study. They showed high values for the entropy rate (around 0.99), and low values for the LZC (ranges from 0.05 to 0.07). However, the degree of predictability and regularity differed between the anatomical directions in some groups of study. For instance, the thin swallows in the non-stroke group, the M-L and S-I directions, related to the sideways and upward movements of the hyolaryngeal structure presented more regular behavior than did the A-P direction, related to the forward movement of the hyolaryngeal structure. Furthermore, the M-L and A-P signals exhibited more predictable behavior and lower LZC than S-I signals in most groups of the study.

In this study, the swallowing signals demonstrated few directional dissimilarities in frequency domain features, which indicates that the energy distribution over the range of the swallowing signal frequencies is approximately the same over the three axes. One of the considerable dissimilarities was the bandwidth of thin swallows in the non-stroke group. The A-P signals in this group presented a wider spread of frequency components than did the S-I signals while showing a narrower spread compared to the M-L signals. Moreover, the M-L signals of the pudding swallows in the stroke group had a higher peak frequency than did the A-P signals, while the A-P signals had higher frequencies than the S-I signals. A higher peak frequency indicates a higher rate of change for a signal.

Lastly, we discussed the results of wavelet entropy which provide information about the relative energy associated with the different frequency bands of the swallowing signals. In this study, the S-I signals demonstrated greater wavelet entropy than the M-L signals in all groups of the study except for the pudding swallows in the stroke group. This means that the signal related to the upward movement of the hyolaryngeal structure during swallowing behaves more disorderly in the time-frequency domain than the sideways movement.

To conclude, we investigated for the first time the existence of swallow vibrations in M-L axis in patients with swallowing difficulties. The results showed that the behavior of swallowing vibrations in M-L axis, representing the sideways movement of the hyolaryngeal structure during the swallowing function, was pretty similar to the behavior of swallowing vibrations in the two other axes. In general, despite few dissimilarities obtained from the directional feature comparisons discussed before in the discussion section, the swallowing signals in all three anatomical directions demonstrated similar behaviors in most computed features and among different groups of our study. Our findings seem to bring the practicability of applying dual/tri-axial accelerometry to the analysis of swallowing signals into question as it suggests that we can make inferences about the behavior of one of the axes based on the other axes by considering the viscosity of the swallows and participant's stroke history. The lack of existence of directional differences in swallowing signals also raises the question of whether the physiological sources of the three axes are dependent upon each other. Further research of swallowing physiology with tri-axial accelerometry using concurrent videofluoroscopic images must be pursued in order to understand the sources of swallowing-related vibrations. In addition, we can only interpenetrates from our results that three directions are similar in most of the computed features without finding out which one would be more successful to classify healthy and unhealthy swallows accurately. Therefore, examining the ability and validity of the three directions to classify swallows would be a valuable investigation as the final goal of swallowing vibratory studies is swallows classification.

Furthermore, the manual segmentation of swallowing signals might increase the rate of human error due to fatigue and decreasing consistency in segmentation criteria, although we have carefully controlled for that by using ongoing reliability testing. Investigating a swallow segmentation algorithm that can extract each swallow from the recorded signals with high accuracy would be an important contribution. Finally, the Mendelsohn or supraglottic swallow maneuver has been used to treat patients with dysphagia for many years, sometimes as a compensatory strategy to help the bolus pass more efficiently through the pharynx, and sometimes as part of a rehabilitative exercise program. It would be good to research the differences between maneuver-mediated swallows and swallows in natural situations in patients with dysphagia, in order to evaluate the effectiveness of rehabilitation programs, and to consider the cervical method as a screening test in rehabilitation centers. Specially previous studies showed the possible effects of neutral head-neck posture and the head-neck flexion (chin-tuck) position on swallowing signals in the A-P and S-I axes [43], [48].

V. Conclusion

In this study, we have compared swallowing accelerometry signals among the anterior-posterior, superior-inferior, and medial-lateral directions in patients with dysphagia. We considered 9 features from 881 swallowing accelerometry signals in various domains including: time, information-theoretic, frequency, and time-frequency domains. The results indicated that movements related to the vibrations emanating from the hyolaryngeal complex in all three directions have similar behavior in most of the extracted features in this study, but there were a few directional differences as well. First, standard deviation, LZC, and wavelet entropy values demonstrated the most directional differences among all the computed features. Secondly, S-I direction showed more complex and irregular behavior with variable amplitude than the M-L and A-P directions. Thirdly, considering viscosity and participant's pathology, thin swallows in the non-stroke group presented the most directional differences among all groups of study.

Acknowledgments

Research reported in this publication was supported by the Eunice Kennedy Shriver National Institute Of Child Health & Human Development of the National Institutes of Health under Award Number R01HD074819. The content is solely the responsibility of the authors and does not necessarily represent the official views of the National Institutes of Health.

References

1. Logemann JA, Logemann JA. Evaluation and treatment of swallowing disorders. Nat Student Speech Language Hearing Assoc J. 1983:38–50.
2. Miller AJ. The neurobiology of swallowing and dysphagia. Dev Disabil Res Rev. 2008; 14(2):77–86. [PubMed: 18646019]
3. Sura L, Madhavan A, Carnaby G, Crary MA. Dysphagia in the elderly: management and nutritional considerations. Clin Interv Aging. 2012; 7(287):98.
4. Chen P-H, Golub JS, Hapner ER, Johns MM III. Prevalence of perceived dysphagia and quality-of-life impairment in a geriatric population. Dysphagia. 2009; 24(1):1–6. [PubMed: 18368451]
5. Chai J, Chu F, Chow T, Shum N. Prevalence of malnutrition and its risk factors in stroke patients residing in an infirmary. Singapore Med J. 2008; 49(4):290. [PubMed: 18418520]
6. Gordon C, Hewer RL, Wade DT. Dysphagia in acute stroke. Br Med J. 1987; 295(6595):411–414. [PubMed: 3115478]
7. Aslam M, Vaezi MF. Dysphagia in the elderly. Gastroenterology & Hepatology. 2013; 9(12):784. [PubMed: 24772045]
8. Rosenthal DI, Lewin JS, Eisbruch A. Prevention and treatment of dysphagia and aspiration after chemoradiation for head and neck cancer. J Clin Oncol. 2006; 24(17):2636–2643. [PubMed: 16763277]
9. Bhattacharyya N. The prevalence of dysphagia among adults in the united states. Otolaryngol Head Neck Surg. 2014; 151(5):765–769. [PubMed: 25193514]
10. Roy N, Stemple J, Merrill RM, Thomas L. Dysphagia in the elderly: preliminary evidence of prevalence, risk factors, and socioemotional effects. Ann Otol Rhinol Laryngol. 2007; 116(11): 858–865. [PubMed: 18074673]
11. Sheth N, Diner WC. Swallowing problems in the elderly. Dysphagia. 1988; 2(4):209–215. [PubMed: 3251696]
12. Schindler JS, Kelly JH. Swallowing disorders in the elderly. The Laryngoscope. 2002; 112(4):589–602. [PubMed: 12150508]

13. Mathers-Schmidt BA, Kurlinski M. Dysphagia evaluation practices: inconsistencies in clinical assessment and instrumental examination decision-making. Dysphagia. 2003; 18(2):114–125. [PubMed: 12825905]
14. Singh S, Hamdy S. Dysphagia in stroke patients. Postgrad Med J. 2006; 82(968):383–391. [PubMed: 16754707]
15. Langmore SE, Kenneth SM, Olsen N. Fiberoptic endoscopic examination of swallowing safety: a new procedure. Dysphagia. 1988; 2(4):216–219. [PubMed: 3251697]
16. Chih-Hsiu W, Tzu-Yu H, Jiann-Chyuan C, Yeun-Chung C, Shiann-Yann L. Evaluation of swallowing safety with fiberoptic endoscope: comparison with videofluoroscopic technique. The Laryngoscope. 1997; 107(3):396–401. [PubMed: 9121321]
17. Reddy NP, Katakam A, Gupta V, Unnikrishnan R, Narayanan J, Canilang EP. Measurements of acceleration during videofluorographic evaluation of dysphagic patients. Med Eng Phys. 2000; 22(6):405–412. [PubMed: 11086251]
18. Wilson RD, Howe EC. A cost-effectiveness analysis of screening methods for dysphagia after stroke. Amer J Phys Med Rehabil. 2012; 4(4):273–282.
19. Zoratto D, Chau T, Steele C. Hyolaryngeal excursion as the physiological source of swallowing accelerometry signals. Physiol Meas. 2010; 31(6):843. [PubMed: 20479519]
20. Zenner PM, Losinski DS, Mills RH. Using cervical auscultation in the clinical dysphagia examination in long-term care. Dysphagia. 1995; 10(1):27–31. [PubMed: 7859529]
21. Cichero JA, Murdoch BE. Detection of swallowing sounds: methodology revisited. Dysphagia. 2002; 17(1):40–49. [PubMed: 11824392]
22. Lee J, Steele C, Chau T. Time and time–frequency characterization of dual-axis swallowing accelerometry signals. Physiol Meas. 2008; 29(9):1105. [PubMed: 18756027]
23. Steele CM, Bailey GL, Chau T, Molfenter SM, Oshalla M, Waito AA, Zoratto DC. The relationship between hyoid and laryngeal displacement and swallowing impairment. Clin Otolaryngol. 2011; 36(1):30–36. [PubMed: 21414151]
24. Perlman A, Palmer P, McCulloch T, Vandaele D. Electromyographic activity from human laryngeal, pharyngeal, and submental muscles during swallowing. J Appl Physiol. 1999; 86(5): 1663–1669. [PubMed: 10233133]
25. Kim Y, McCullough GH. Maximum hyoid displacement in normal swallowing. Dysphagia. 2008; 23(3):274–279. [PubMed: 17962998]
26. Lazareck, L., Moussavi, Z. The 26th Ann Int Conf IEEE Eng Med Biol Soc. Vol. 2. San Francisco, CA: Sep 1–5. 2004 Swallowing sound characteristics in healthy and dysphagic individuals; p. 3820-3823.
27. Yadollahi, A., Moussavi, Z. The 29th Ann Int Conf IEEE Eng Med Biol Soc. Lyon, FR: Aug 22–26. 2007 Feature selection for swallowing sounds classification; p. 3172-3175.
28. Youmans S, Stierwalt J. Normal swallowing acoustics across age, gender, bolus viscosity, and bolus volume. Dysphagia. Dec; 2011 26(4):374–384. [PubMed: 21225287]
29. Youmans S, Stierwalt J. An acoustic profile of normal swallowing. Dysphagia. Sep; 2005 20(3): 195–209. [PubMed: 16362508]
30. Takahashi K, Groher M, Michi K. Symmetry and reproducibility of swallowing sounds. Dysphagia. Sep; 1994 9(3):168–173. [PubMed: 8082325]
31. Lee J, Steele CM, Chau T. Classification of healthy and abnormal swallows based on accelerometry and nasal airflow signals. Artif Intell Med. 2011; 52(1):17–25. [PubMed: 21549579]
32. Nikjoo MS, Steele CM, Sejdić E, Chau T. Automatic discrimination between safe and unsafe swallowing using a reputation-based classifier. Biomed Eng OnLine. 2011; 10(1):100. [PubMed: 22085802]
33. Dudik JM, Kurosu A, Coyle JL, Sejdić E. A comparative analysis of dbscan, k-means, and quadratic variation algorithms for automatic identification of swallows from swallowing accelerometry signals. Comput Biol Med. 2015; 59:10–18. [PubMed: 25658505]
34. Dudik JM, Coyle JL, Sejdic E. Dysphagia screening: Contributions of cervical auscultation signals and modern signal-processing techniques. IEEE Trans Human Mach Syst. 2015; 45(4):465–477.

35. Lee J, Steele CM, Chau T. Swallow segmentation with artificial neural networks and multi-sensor fusion. Med Eng Phys. 2009; 31(9):1049–1055. [PubMed: 19646911]
36. Sejdić E, Steele CM, Chau T. Understanding the statistical persistence of dual-axis swallowing accelerometry signals. Comput Biol Med. 2010; 40(11):839–844. [PubMed: 21035113]
37. Sejdić E, Komisar V, Steele CM, Chau T. Baseline characteristics of dual-axis cervical accelerometry signals. Ann Biomed Eng. 2010; 38(3):1048–1059. [PubMed: 20336838]
38. Dudik JM, Jestrović I, Luan B, Coyle JL, Sejdić E. A comparative analysis of swallowing accelerometry and sounds during saliva swallows. Biomed Eng Online. Jan; 2015 14(3):1–15. [PubMed: 25564100]
39. Atkins BZ, Trachtenberg MS, Prince-Petersen R, Vess G, Bush EL, Balsara KR, Lin SS, Davis RD. Assessing oropharyngeal dysphagia after lung transplantation: altered swallowing mechanisms and increased morbidity. J Heart Lung Transplant. 2007; 26(11):1144–1148. [PubMed: 18022080]
40. Tabaee A, Murry T, Zschommler A, Desloge RB. Flexible endoscopic evaluation of swallowing with sensory testing in patients with unilateral vocal fold immobility: incidence and pathophysiology of aspiration. The Laryngoscope. 2005; 115(4):565–569. [PubMed: 15805859]
41. Ayuse T, Ishitobi S, Kurata S, Sakamoto E, Okayasu I, Oi K. Effect of reclining and chin-tuck position on the coordination between respiration and swallowing. J Oral Rehabil. 2006; 33(6):402–408. [PubMed: 16671985]
42. Takahashi K, Groher ME, Michi K. Methodology for detecting swallowing sounds. Dysphagia. 1994; 9(1):54–62. [PubMed: 8131426]
43. Jestrovic I, Dudik JM, Luan B, Coyle JL, Sejdić E. The effects of increased fluid viscosity on swallowing sounds in healthy adults. Biomedl Eng OnLine. 2013; 12(1):90.
44. Holas MA, DePippo KL, Reding MJ. Aspiration and relative risk of medical complications following stroke. Arch Neurol. 1994; 51(10):1051–1053. [PubMed: 7945003]
45. Smithard D, Smeeton N, Wolfe C. Long-term outcome after stroke: does dysphagia matter? Age Ageing. 2007; 36(1):90–94. [PubMed: 17172601]
46. Lee J, Sejdić E, Steele CM, Chau T, et al. Effects of liquid stimuli on dual-axis swallowing accelerometry signals in a healthy population. Biomed Eng OnLine. 2010; 9(7)
47. Sejdić E, Steele CM, Chau T. A method for removal of low frequency components associated with head movements from dual-axis swallowing accelerometry signals. PLoS One. 2012; 7(3):e33464. [PubMed: 22479402]
48. Sejdić E, Steele CM, Chau T. The effects of head movement on dual-axis cervical accelerometry signals. BMC Res Notes. 2010; 3(1):269. [PubMed: 20977753]
49. Sejdić E, Steele CM, Chau T. A procedure for denoising dual-axis swallowing accelerometry signals. Physiol Meas. 2010; 31(1):N1. [PubMed: 19940343]
50. Sejdić E, Lowry KA, Bellanca J, Redfern MS, Brach JS. A comprehensive assessment of gait accelerometry signals in time, frequency and time-frequency domains. IEEE Trans Neural Syst Rehabil Eng. 2014; 22(3):603–612. [PubMed: 23751971]
51. DeCarlo LT. On the meaning and use of kurtosis. Psychol Methods. 1997; 2(3):292.
52. Aboy M, Hornero R, Abásolo D, Álvarez D. Interpretation of the lempel-ziv complexity measure in the context of biomedical signal analysis. IEEE Trans Biomed Eng. 2006; 53(11):2282–2288. [PubMed: 17073334]
53. Hu J, Gao J, Principe JC. Analysis of biomedical signals by the lempel-ziv complexity: the effect of finite data size. IEEE Trans Biomed Eng. 2006; 53(12):2606–2609. [PubMed: 17152441]
54. Porta A, Guzzetti S, Montano N, Furlan R, Pagani M, Malliani A, Cerutti S. Entropy, entropy rate, and pattern classification as tools to typify complexity in short heart period variability series. IEEE Trans Biomed Eng. 2001; 48(11):1282–1291. [PubMed: 11686627]
55. Porta A, Baselli G, Liberati D, Montano N, Cogliati C, Gnecchi-Ruscone T, Malliani A, Cerutti S. Measuring regularity by means of a corrected conditional entropy in sympathetic outflow. Biol Cybern. 1998; 78(1):71–78. [PubMed: 9485587]
56. Kumar Y, Dewal ML, Anand RS. Relative wavelet energy and wavelet entropy based epileptic brain signals classification. Biomed Eng Lett. 2012; 2(3):147–157.

57. Quiroga RQ, Rosso OA, Ba¸sar E, Schürmann M. Wavelet entropy in event-related potentials: a new method shows ordering of EEG oscillations. Biol Cybern. 2001; 84(4):291–299. [PubMed: 11324340]

58. Natwong, B., Sooraksa, P., Pintavirooj, C., Bunluechokchai, S., Ussawawongaraya, W. Proc of the 1st IEEE Conf on Ind Electron and Applicat. Singapore: May 24–26. 2006 Wavelet entropy analysis of the high resolution ECG; p. 1-4.

59. Sejdić E, Djurović I, Jiang J. Time–frequency feature representation using energy concentration: An overview of recent advances. Digit Signal Process. 2009; 19(1):153–183.

60. Rosso OA, Blanco S, Yordanova J, Kolev V, Figliola A, Schürmann M, Başar E. Wavelet entropy: a new tool for analysis of short duration brain electrical signals. J Neurosci Methods. 2001; 105(1): 65–75. [PubMed: 11166367]

61. McKee G, Johnston B, McBride G, Primrose W. Does age or sex affect pharyngeal swallowing? Clin Otolaryngol Allied Sci. 1998; 23(2):100–106. [PubMed: 9597278]

62. Ekberg O, Wahlgren L. Dysfunction of pharyngeal swallowing a cineradiographic investigation in 854 dysphagial patients. Acta Radiol Diagn. 1985; 26(4):389–395.

63. Sejdić E, Steele CM, Chau T. Segmentation of dual-axis swallowing accelerometry signals in healthy subjects with analysis of anthropometric effects on duration of swallowing activities. IEEE Trans Biomed Eng. 2009; 56(4):1090–1097. [PubMed: 19171514]

64. Kuhl V, Eicke B, Dieterich M, Urban P. Sonographic analysis of laryngeal elevation during swallowing. J Neurol. 2003; 250(3):333–337. [PubMed: 12638025]

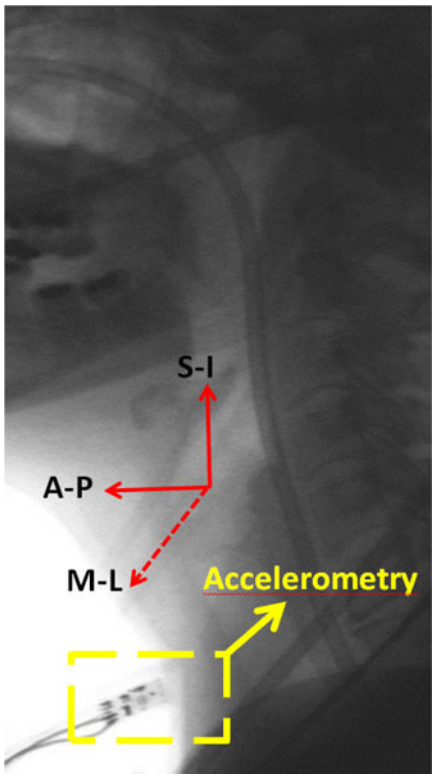

Fig. 1.
Location of the sensor on a participant's neck and orientation of the three anatomical axes of the sensor.

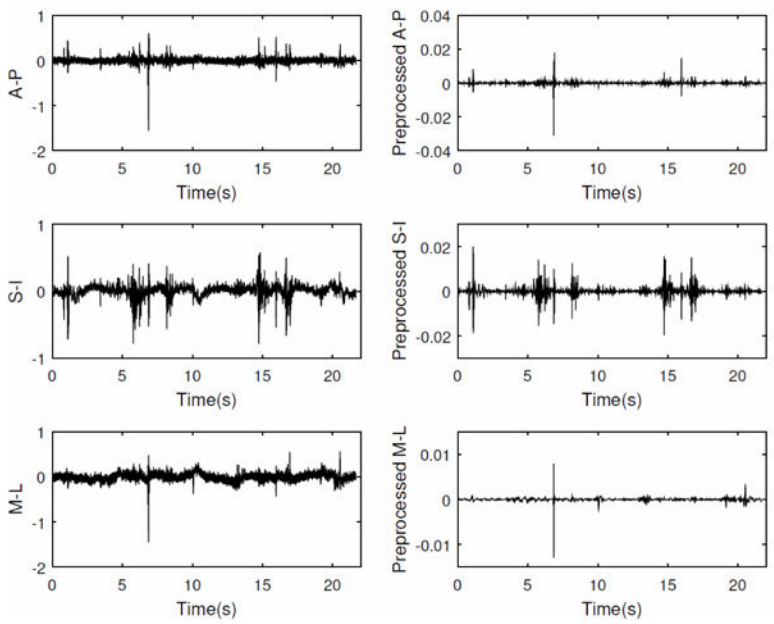

Fig. 2.

Recorded swallow vibrations in three axes of accelerometer before and after applying signal processing techniques.

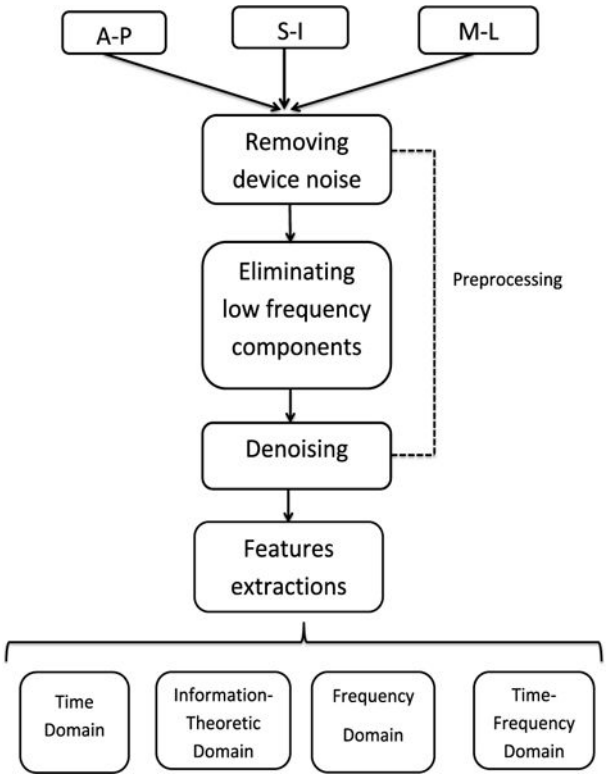

Fig. 3.
Flowchart outlining preprocessing and feature extraction steps.

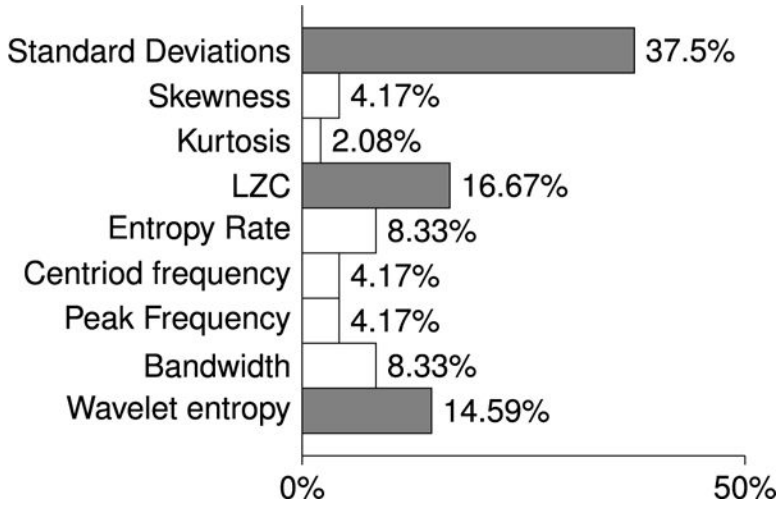

Fig. 4.

The percentages of dissimilarities between the axes of the swallowing accelerometer for each of the computed features are calculated by dividing the number of cases found to exhibit dissimilarities by the total number of comparisons made for each of the computed features.

TABLE 1

Summary of All Features

Time Domain Features	
Standard deviation (σ)	Reflects how a signal fluctuates around the mean value of a signal.
Skewness (ξ)	Describes the asymmetry of the amplitude distribution. Negative and positive skewness indicates the distribution of the signal with a long tail, higher values, to the left/right side.
Kurtosis (γ)	Describes peaked/flat amplitude distribution relative to a normal distribution. High/low kurtosis values specify a signal distribution with a sharp/flattened peak.
Information-Theoretic Domain Features	
Lempel-Ziv Complexity (LZC)	Evaluates the randomness of a signal. Higher/lower values indicate more/less randomness in the signal.
Entropy rate (ρ)	Evaluates the degree of regularity of the signal distribution. Zero and one entropy rate indicates a periodic repetition of the same pattern and aperiodic dynamics, respectively.
Frequency Domain Features	
Peak frequency (f)	Describes the frequency corresponding to the maximum spectral power.
Spectral centroid $(\hat{f})$	The frequency that divides the spectral power into two equal parts.
Bandwidth (BW)	The difference between the uppermost and lowermost frequencies in a signal.
Time-Frequency Domain Features	
Wavelet entropy (Θ_X)	Evaluates the disorderly behavior in time-frequency domain. High and low values of wavelet entropy specify disorder/order behavior in a signal.

IEEE Trans Neural Syst Rehabil Eng. Author manuscript; available in PMC 2018 May 01.

TABLE 2

Time-domain features (mean ± standard deviation) extracted from the three anatomical axes of swallowing signals grouped by the participants' stroke history and viscosity

		Stroke			Non-Stroke		
		$\sigma_s(g) * 10^{-2}$	ξ_s	$\gamma_s * 10^2$	$\sigma_{ns}(g) * 10^{-2}$	ξ_{ns}	$\gamma_{ns} * 10^2$
Thin	A-P	$0.16 \pm 0.13^{\S\dagger}$	0.55 ± 4.88	1.66 ± 7.92	$0.19 \pm 0.19^{\S\dagger}$	$0.72 \pm 2.55^{\S}$	0.37 ± 0.75
	S-I	$0.29 \pm 0.22^{\S\ddagger}$	-0.47 ± 1.60	0.18 ± 0.30	$0.31 \pm 0.21^{\S\ddagger}$	$-0.57 \pm 2.69^{\S}$	0.42 ± 1.50
	M-L	$0.06 \pm 0.04^{\dagger\ddagger}$	0.71 ± 3.53	0.30 ± 1.75	$0.07 \pm 0.07^{\dagger\ddagger}$	0.31 ± 3.42	0.61 ± 4.46
Nectar	A-P	$0.15 \pm 0.20^{\S\dagger}$	-0.09 ± 4.57	1.48 ± 8.37	$0.16 \pm 0.20^{\S\dagger}$	0.73 ± 2.24	0.49 ± 1.10
	S-I	$0.24 \pm 0.19^{\S\ddagger}$	-0.30 ± 1.34	0.15 ± 0.24	$0.28 \pm 0.23^{\S\ddagger}$	0.14 ± 4.37	0.71 ± 2.90
	M-L	$0.06 \pm 0.04^{\dagger\ddagger}$	0.13 ± 1.14	0.13 ± 0.33	$0.06 \pm 0.05^{\dagger\ddagger}$	0.64 ± 3.57	0.78 ± 3.79
Puddung	A-P	$0.10 \pm 0.05^{\S\dagger}$	-1.40 ± 4.79	1.83 ± 7.96	$0.18 \pm 0.14^{\S\dagger}$	$1.12 \pm 3.21^{\S}$	$0.55 \pm 0.99^{\S}$
	S-I	$0.20 \pm 0.11^{\S\ddagger}$	-0.13 ± 0.74	0.06 ± 0.07	$0.27 \pm 0.18^{\S\ddagger}$	$-0.05 \pm 1.87^{\S}$	$0.24 \pm 0.46^{\S}$
	M-L	$0.05 \pm 0.03^{\dagger\ddagger}$	0.20 ± 1.07	0.08 ± 0.21	$0.08 \pm 0.10^{\dagger\ddagger}$	0.05 ± 0.45	0.41 ± 1.58

σ = Standard deviation, ξ = Skewness, γ = Kurtosis

†= Statistical difference between A-P and M-L axes

‡= Statistical difference between S-I and M-L axes

§= Statistical difference between A-P and S-I axes

Values were statistically significant when probability is less than 0.05 (*p-value* < 0.05).

IEEE Trans Neural Syst Rehabil Eng. Author manuscript; available in PMC 2018 May 01.

TABLE 3

Information-theoretic features (mean ± standard deviation) extracted from the three anatomical axes of swallowing signals grouped by the participants' stroke history and viscosity

		Stroke		Non-Stroke	
		LZC_S	$\rho_s * 10^{-1}$	LZC_{ns}	$\rho_{ns} * 10^{-1}$
Thin	A-P	0.05 ± 0.02§	9.86 ± 0.01	0.06 ± 0.02	9.86 ± 0.01§†
	S-I	0.06 ± 0.02§	9.87 ± 0.01	0.07 ± 0.02‡	9.88 ± 0.00§‡
	M-L	0.06 ± 0.02	9.89 ± 0.00	0.06 ± 0.02‡	9.89 ± 0.00†‡
Nectar	A-P	0.06 ± 0.03§	9.89 ± 0.01	0.06 ± 0.02	9.88 ± 0.01†
	S-I	0.07 ± 0.02§‡	9.89 ± 0.00	0.06 ± 0.03	9.89 ± 0.00
	M-L	0.06 ± 0.02‡	9.89 ± 0.00	0.06 ± 0.02	9.90 ± 0.00†
Puddung	A-P	0.06 ± 0.03	9.90 ± 0.00	0.05 ± 0.02§	9.88 ± 0.00
	S-I	0.07 ± 0.02‡	9.89 ± 0.00	0.07 ± 0.03§‡	9.89 ± 0.00
	M-L	0.05 ± 0.02‡	9.90 ± 0.00	0.06 ± 0.02‡	9.89 ± 0.00

LZC= Lempel-Ziv Complexity, ρ= Entropy rate

†= Statistical difference between A-P and M-L axes

‡= Statistical difference between S-I and M-L axes

§= Statistical difference between A-P and S-I axes

Values were statistically significant when probability is less than 0.05 (*p-value* < 0.05).

IEEE Trans Neural Syst Rehabil Eng. Author manuscript; available in PMC 2018 May 01.

TABLE 4

Frequency features (mean ± standard deviation) extracted from the three anatomical axes of swallowing signals grouped by the participants' stroke history and viscosity

		Stroke			Non-Stroke		
		$f_s(Hz)*10^2$	$\hat{f}_s(Hz)*10^3$	$BW_s(Hz)*10^2$	$f_{ns}(Hz)*10^2$	$\hat{f}_{ns}(Hz)*10^2$	$BW_{ns}(Hz)*10^2$
Thin	A-P	0.20 ± 0.68	0.41 ± 1.15	4.22 ± 5.75†	0.15 ± 0.42	1.19 ± 2.12	2.10 ± 3.53§†
	S-I	0.11 ± 0.11	0.08 ± 0.07‡	1.46 ± 1.46	0.12 ± 0.27	0.96 ± 3.91	1.45 ± 3.38§
	M-L	0.06 ±0.11	0.04 ± 0.10‡	0.98 ± 1.61†	0.08 ± 0.23	0.95 ± 4.66	1.16 ± 3.30†
Nectar	A-P	1.06 ± 8.04	0.29 ± 0.96	3.38 ± 6.12	0.08 ± 0.20	1.72 ± 3.42	3.22 ± 5.33†
	S-I	0.12 ± 0.28	0.04 ± 0.06	1.01 ± 1.42	0.12 ± 0.43	1.16 ± 3.98	1.90 ± 3.92
	M-L	0.06 ± 0.13	0.03 ± 0.06	0.81 ± 1.02	0.06 ± 0.08	1.01 ± 4.80	1.24 ± 3.95†
Pudding	A-P	0.03 ± 0.02§†	0.29 ± 1.22	2.50 ± 6.25	0.12 ± 0.36	1.41 ± 2.28§	2.67 ± 3.62
	S-I	0.06 ± 0.02§	0.03 ± 0.04	0.80 ± 1.57	0.09 ± 0.09	0.96 ± 2.07§	2.06 ± 4.07
	M-L	0.05 ± 0.03†	0.02 ± 0.03	1.35 ± 1.93	0.08 ± 0.18	1.19 ± 4.17	2.05 ± 5.66

f = Peak frequency, $\hat{f}$ = Spectral centroid, BW = Bandwidth

†= Statistical difference between A-P and M-L axes

‡= Statistical difference between S-I and M-L axes

§= Statistical difference between A-P and S-I axes

Values were statistically significant when probability is less than 0.05 (p-*value* < 0.05).

TABLE 5

Time-frequency features (mean ± standard deviation) extracted from the three anatomical axes of swallowing signals grouped by the participants' stroke history and viscosity

		Stroke	Non-Stroke
		Θ_{X_s}	$\Theta_{X_{ns}}$
Thin	A-P	1.07 ± 0.85	1.09 ± 0.81†
	S-I	1.02 ± 0.74‡	1.19 ± 0.73‡
	M-L	0.53 ± 0.59‡	0.68 ± 0.69†‡
Nectar	A-P	0.73 ± 0.75§	1.01 ± 0.83†
	S-I	0.83 ± 0.70§	1.11 ± 0.77‡
	M-L	0.48 ± 0.52	0.67 ± 0.66†‡
Pudding	A-P	0.62 ± 0.64	0.91 ± 0.75
	S-I	0.67 ± 0.56	0.99 ± 0.75‡
	M-L	0.34 ± 0.31	0.67 ± 0.78‡

Θ_X = Wavelet entropy

†= Statistical difference between A-P and M-L axes

‡= Statistical difference between S-I and M-L axes

§= Statistical difference between A-P and S-I axes

Values were statistically significant when probability is less than 0.05 (*p-value* < 0.05).

IEEE Trans Neural Syst Rehabil Eng. Author manuscript; available in PMC 2018 May 01.

TABLE 6

Summary of directional differences among groups of study. all dots (red and black dots) indicate the existence of directional dissimilarities, which means the p-value of the comparison is statistically significant at the $p<0.05$ level. The “axes” column demonstrates which two axes are compared to each other. Red dots indicate that first axis in the “axes” column has a higher value of the computed feature in “Features” column than does the second axis, while black dots indicate the second axis has a higher value than the first axis.

		stroke			Non-stroke		
Features	**Axes**	**Thin**	**Nectar**	**Pudding**	**Thin**	**Nectar**	**Pudding**
Standard Deviation	A-P & S-I	●	●	●	●	●	●
	A-P & M-L	●	●	●	●	●	●
	M-L & S-I	●	●	●	●	●	●
Skewness	A-P & S-I				●		●
	A-P & M-L						
	M-L & S-I						
Kurtosis	A-P & S-I						●
	A-P & M-L						
	M-L & S-I						
LZC	A-P & S-I	●	●				●
	A-P & M-L						
	M-L & S-I		●	●	●		●
Entropy Rate	A-P & S-I				●		
	A-P & M-L				●	●	
	M-L & S-I				●		
Centroid Frequency	A-P & S-I						●
	A-P & M-L						
	M-L & S-I	●					
Peak Frequency	A-P & S-I			●			

Features	Axes	stroke			Non-stroke		
		Thin	Nectar	Pudding	Thin	Nectar	Pudding
	A-P & M-L			●			
	M-L & S-I						
Bandwidth	A-P & S-I				●		
	A-P & M-L	●			●	●	
	M-L & S-I						
Wavelet Entropy	A-P & S-I		●				
	A-P & M-L				●	●	
	M-L & S-I	●			●	●	●